



Cite this: Dalton Trans., 2023, 52, 17928

Received 16th August 2023,  
Accepted 20th October 2023  
DOI: 10.1039/d3dt02664g  
[rsc.li/dalton](http://rsc.li/dalton)

## Bis(tetrelocenes) – fusing tetrelocenes into close proximity†

Inga-Alexandra Bischoff,<sup>a</sup> Bernd Morgenstern,<sup>a</sup> Michael Zimmer,<sup>a</sup> Aylin Koldemir,<sup>b</sup> Rainer Pöttgen<sup>ID, b</sup> and André Schäfer<sup>ID, \*a</sup>

We report the synthesis and structure of two bis(germanocenes) and a bis(stannocene), obtained by the reaction of unsymmetric *ansa* bis(cyclopentadienyl) ligands with germanium and tin dichloride. DFT calculations show that the formation of these bis(tetrelocenes) is energetically favoured over the formation of the corresponding [1]tetrelcenophanes. In the crystal structure authenticated structural motif, the two tetrel(II) centers are forced into close proximity to each other, resulting in weak donor–acceptor interactions, according to Natural Bond Orbital (NBO) and Atoms in Molecules (AIM) analyses.

### Introduction

The report of the famous  $[(\text{Me}_3\text{Si})_2\text{CH}]_2\text{Sn}$  stannylene by Lappert *et al.* in 1973 marks a milestone in low-valent group 14 chemistry.<sup>1</sup> In the solid state, this compound possesses a dimeric distannene-type structure, and thus exhibits a homonuclear double bond between the heavier group 14 elements (Fig. 1).<sup>2</sup> This finding refutes earlier assumptions that the formation of multiple bonds between heavier main group elements (starting with elements of the third period) is not possible due to poor orbital overlap, a principle that came to be known as the “double bond rule”.<sup>3</sup> Around the same time, the analogous germanium and lead species were also reported, and they also possess dimeric structures in the solid state.<sup>1,2b,4</sup> Nowadays, numerous examples of heavy ditetrelenes of germanium, tin and lead exist.<sup>5</sup> In many cases, these species can monomerize into the corresponding tetrylene fragments in solution and in the gas phase, owing to their relatively weak element–element double bonds, and influenced by the steric demand of their substituents.<sup>4,5p,r,t,6</sup> On the other hand, amido-substituted tetrylenes usually do not form ditetrelene-type aggregates,<sup>4a,7</sup> due to their electronic stabilization.

Another class of tetrylene-type compounds, with the general formula “ $\text{R}_2\text{E}$ ”, are tetrelocenes (group 14 metalloc-

cenes) bearing  $\eta^5$ -coordinated cyclopentadienyl ligands (Fig. 1).<sup>8</sup> The first reports of tetrelocenes date back to 1956, when Fischer *et al.* reported stannocene and plumbocene.<sup>9</sup> Completing this heavy tetrel series, Curtis *et al.* reported germanocene in 1973.<sup>10</sup> Interestingly, although dimers/oligomers of tetrelocene-type species are known in the form of cationic multi-decker complexes,<sup>11</sup> tetrelocenes do not form dimers with  $\text{E}=\text{E}$  double bonds, although the steric demand of the cyclopentadienyl groups is comparatively small. The reason is of an energetic nature, since tetrelocenes exhibit only limited acceptor properties and no significant donor strength, as the lone pair is of very high s character and is correspondingly low in energy.<sup>8,12</sup>

To investigate if it is possible to induce bonding interactions between two tetrelocene moieties, we explored the

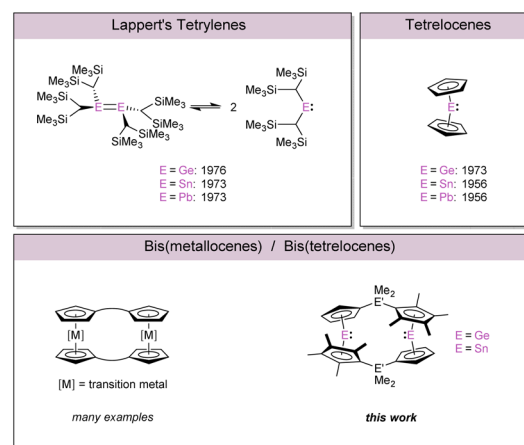


Fig. 1 Overview of selected tetrylenes, tetrelocenes and bis (metallocenes).

<sup>a</sup>Department of Chemistry, Faculty of Natural Sciences and Technology, Saarland University, Campus Saarbrücken, 66123 Saarbrücken, Germany.

E-mail: [andre.schaefer@uni-saarland.de](mailto:andre.schaefer@uni-saarland.de)

<sup>b</sup>Institute of Inorganic and Analytical Chemistry, Faculty of Chemistry and Pharmacy, University of Münster, Corrensstrasse 30, 48149 Münster, Germany

†Electronic supplementary information (ESI) available: NMR spectra, Mössbauer spectra, XRD data, IR spectra, UV-Vis spectra, computational details and references. CCDC 2288211–2288213. For ESI and crystallographic data in CIF or other electronic format see DOI: <https://doi.org/10.1039/d3dt02664g>



possibility to interlink two tetrelenes, by introducing  $\text{Me}_2\text{Si}$  and  $\text{Me}_2\text{Ge}$  bridging units, effectively forcing the metal centers to come in close proximity to each other. The structural motif of such bis(metallocenes) is known in transition metal chemistry (Fig. 1), where such compounds exhibit a variety of different linkers,<sup>13</sup> but is very rare for main group elements.<sup>14</sup>

## Results and discussion

We chose to employ two different, asymmetric *ansa* ligands in our study, a sila[1]- and the corresponding germa[1]-bridged system, both carrying a cyclopentadienyl (Cp) and a tetramethyl-cyclopentadienyl (Cp<sup>#</sup>) group. Treatment of the dilithiated form of the sila[1]-ligand, **1a**, with tin(II) chloride and a germanium(II) chloride dioxane adduct, and of the dilithiated germa[1]-ligand, **1b**, with germanium(II) chloride dioxane in THF at room temperature, afforded the corresponding bis(tetrelenes) **2a–c** (Scheme 1). The bis(stannocene) **2c** exhibits a <sup>119</sup>Sn NMR chemical shift of  $\delta^{119}\text{Sn}\{^1\text{H}\} = -2138$  in solution, which is within the common chemical shift range of stannocene-type compounds ( $\delta^{119}\text{Sn}(\text{Cp}_2\text{Sn}) = -2199$ ,<sup>15</sup>  $\delta^{119}\text{Sn}(\text{Cp}^*\text{Sn}) = -2129$ <sup>15</sup>). Furthermore, the solid-state <sup>119</sup>Sn{<sup>1</sup>H}(CP/MAS) NMR spectrum of **2c** reveals a quasi-identical resonance at -2139 ppm, indicating that the solid-state structure is persistent in solution.<sup>16</sup> Single crystals of **2a–c** suitable for X-ray diffraction could be obtained from hexane/THF mixtures and allowed for structural characterization in the solid state (Fig. 2 and Fig. S12–S14†). Bis(germanocenes) **2a** and **2b** crystallize in the monoclinic space group *C*2 and bis(stannocene) **2c** in the orthorhombic space group *Aba*2, with the Cp and Cp<sup>#</sup> rings coordinated in a distorted  $\eta^5$  fashion to the metal centers in all cases (Tables S2 and S3†). As per the asymmetric nature of the ligand system, the E–Cp and E–Cp<sup>#</sup> bond lengths are different, with the more electron rich Cp<sup>#</sup> group exhibiting shorter bonds to the tetrel(II) centers.

The Ge–Cp<sup>cent</sup> and Ge–Cp<sup>#cent</sup> distances in **2a–c** are slightly longer than those in previously reported Si[2]germanocenophanes and Si[2]stannocenophanes.<sup>17,18</sup> The most interesting structural feature in bis(tetrelenes) **2a–c** is of course the E–E distances (**2a**: 361.5(6) pm; **2b**: 363.7(6) pm; and **2c**: 367.9(5) pm). In all cases, these distances are much longer than what is typically found in heavy ditetrelenes (Ge=Ge double bond dis-

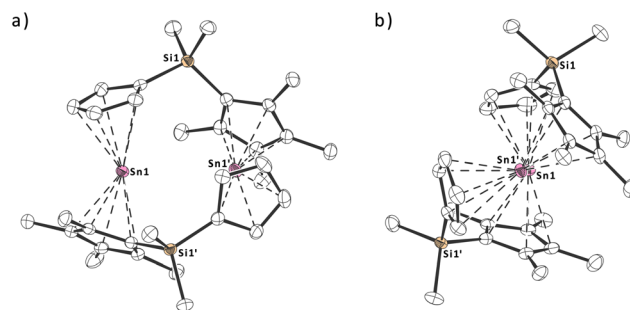
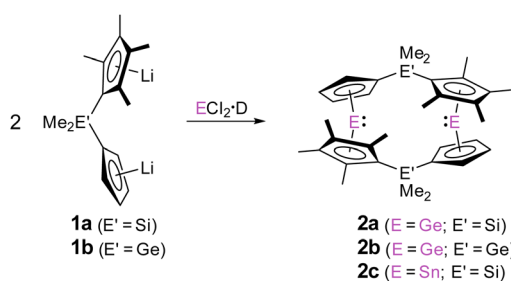


Fig. 2 Molecular structure of **2c** in the crystal, (a) view orthogonal to the Sn1 Sn1' axis, (b) view along the Sn1 Sn1' axis (displacement ellipsoids at a 50% probability level; hydrogen atoms are omitted for clarity).

tances: 221.2(1) pm to 245.4(2) pm;<sup>4,5</sup> Sn=Sn double bond distances: 276.8(7) pm to 291.0(1) pm<sup>5</sup>), indicating that no “classical” double bonds are formed, but are still smaller than the sum of the van der Waals radii ( $\sum r_w(\text{Ge}) = 422$  pm;<sup>19</sup>  $\sum r_w(\text{Sn}) = 434$  pm<sup>19</sup>). For comparison, the  $[\text{2,4,6-(CF}_3\text{)}_3\text{C}_6\text{H}_5]_2\text{Sn}$  stannylene had previously been described to exhibit a dimeric structure in the solid-state with a very long Sn–Sn distance of 363.9 (1) pm,<sup>5i</sup> which is *ca.* 4 pm shorter than what is found in **2c** (367.9(1) pm). Even though the  $\text{Me}_2\text{Ge}$  bridging motif is larger than the  $\text{Me}_2\text{Si}$  bridging motif, the Ge–Ge distance in **2b** is only marginally longer than that in **2a** (Table 1), which might point to a weak Ge–Ge interaction. Noteworthily, the two tetrelene fragments in **2a–c** do not adopt typical trans-bent arrangements but are heavily twisted against each other with torsion angles of  $\tau = 73.9^\circ$ – $82.4^\circ$ , again indicating that there are no classical  $\pi$ -type double bond interactions between the metal centers (Table 1). In addition, <sup>119</sup>Sn Mössbauer spectroscopy of **2c** is indicative of a classical stannocene center (Fig. 3, S11 and Table S1†), with the isomer shift of  $\delta = 3.611$  (3) mm s<sup>-1</sup> and the electric quadrupole splitting of  $\Delta E_Q = 0.70$  (1) mm s<sup>-1</sup> being similar to those of stannocene ( $\delta(\text{Cp}_2\text{Sn}) = 3.73(6)$  mm s<sup>-1</sup>,<sup>20</sup>  $\Delta E_Q = 0.65(6)$  mm s<sup>-1</sup><sup>20</sup>). Noteworthily, the experimental spectrum is well reproduced with three sub-signals, whereby signal A with the highest intensity can be assigned to **2c**, while signals B ( $\text{Sn}^{\text{IV}}$ ) and C ( $\text{Sn}^{\text{II}}$ ) most likely originate from partial decomposition of the sample.<sup>21,22</sup> To further investigate why these bis(tetrelene)-structures formed and to better understand the nature of interactions between the two tetrelene moieties in **2a–c**, we performed DFT calculations.<sup>21</sup> A comparison of the ground-state energies



Scheme 1 Synthesis of bis(tetrelenes) **2a–c**.

Table 1 Selected bond lengths [pm] and angles [°] in **2a–c**

	E–E [pm]	$\alpha$ [°]	$\delta$ [°]	$\tau$ [°]
<b>2a</b>	361.51(6) (E=Ge)	42.2	147.7	73.9
<b>2b</b>	363.74(6) (E=Ge)	43.7	153.7	75.3
<b>2c</b>	367.88(5) (E=Sn)	44.5	154.3	82.4

$\alpha$ : dihedral angle between Cp planes.  $\delta$ :  $\text{Cp}^{\text{centroid}}\text{–E–Cp}^{\text{centroid}}\text{–E}$  angle.  $\tau$ : torsion angle between  $\text{Cp}^{\text{centroid}}\text{–E–E–Cp}^{\text{#centroid}}$ .

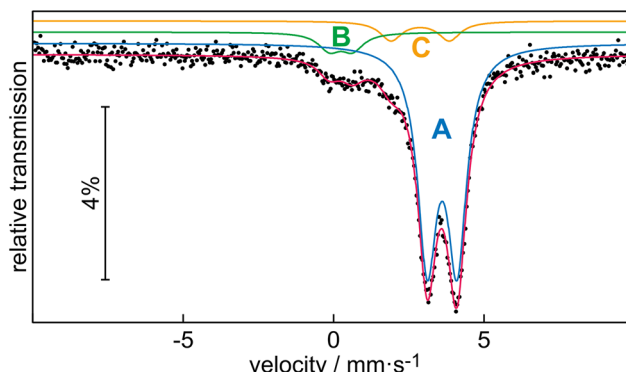


Fig. 3 Experimental and simulated  $^{119}\text{Sn}$  Mössbauer spectrum of **2c** (78 K data).

of **2a–c** to the theoretical [1]tetrelcenophanes shows that the latter are more than 100  $\text{kJ mol}^{-1}$  higher in energy. Similarly, theoretical trans-bent dimers of the [1]tetrelcenophanes are more than 70  $\text{kJ mol}^{-1}$  higher in energy than the experimentally observed structures, **2a–c** (Fig. 4). This may be a consequence of the [1]tetrelcenophanes exhibiting a high degree of ring strain. Inspection of the frontier orbitals does not reveal any  $\pi$  type bonding interaction between the tetrelocene central atoms (Fig. S15–S17†), rather the frontier orbitals are typical of tetrelcenes.<sup>8a</sup>

Furthermore, Natural Bond Orbital (NBO) analysis of **2a–c** reveals that the lone pairs at the central atoms have a high s character (**2a**: 96.9%; **2b**: 96.7%; and **2c**: 98.4%). The interaction between the lone pair of one tetrelocene central atom and the vacant p orbital of the second tetrelocene central atom amounts to 13.0  $\text{kJ mol}^{-1}$  for **2a**, 13.8  $\text{kJ mol}^{-1}$  for **2b**, and 78.7  $\text{kJ mol}^{-1}$  for **2c**; thus **2c** exhibits by far the strongest interaction. This is a result of the larger size of tin compared to that of germanium and thus the Sn–Sn distance is closer to typical Sn–Sn bonds. Furthermore, **2a–c** were studied using the Atoms in Molecules (AIM) method. In all cases, bond critical points (bcp) with very small positive Laplacian values were found, which indicate very weak donor–acceptor interactions (Fig. 5). The strongest interaction between the two central atoms is observed in **2c**, which is in line with the NBO analysis discussed earlier.

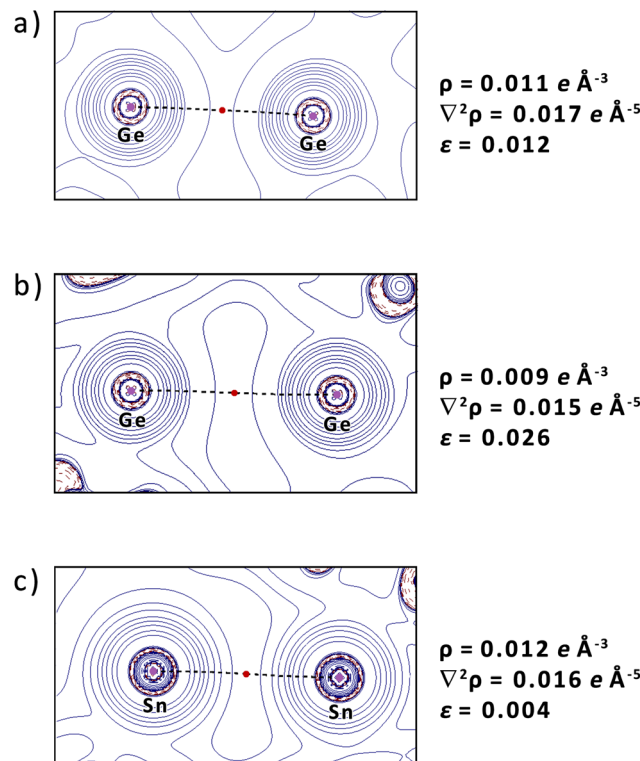


Fig. 5 2D Laplacian distribution  $\nabla^2\rho(r)$  of (a) **2a**, (b) **2b** and (c) **2c** (dashed red lines show areas of charge concentration ( $\nabla^2\rho(r) < 0$ ), solid blue lines show areas of charge depletion ( $\nabla^2\rho(r) > 0$ ), dashed black lines are bond paths, and red dots are bond critical points).

## Conclusions

In conclusion, we were able to synthesize and structurally characterize three bis(tetrelcenes), **2a–c**, in which the cyclopentadienyl substituents are interlinked *via*  $\text{Me}_2\text{Si}$  or  $\text{Me}_2\text{Ge}$  bridging units. This structural motif fused the group 14 metal centers to be in close proximity to each other. DFT calculations confirm that the formation of bis(tetrelcenes) is energetically favoured over tetrelcenophane structures. Additionally, although tetrelcenes do not form ditetrelene-type aggregates, Natural Bond Orbital and Atoms in Molecules analyses demonstrate weak donor–acceptor interactions between the metal centers in **2a–c**, whereby bis(stannocene) **2c** exhibits the strongest interaction between its tin centers.

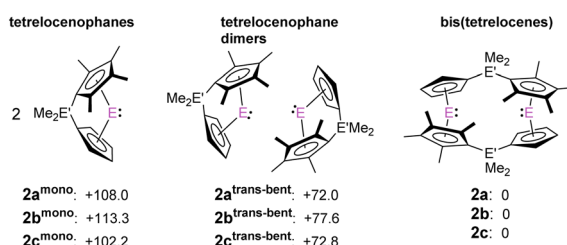


Fig. 4 Relative energies of theoretical [1]tetrelcenophanes, trans-bent dimers, and the experimentally observed bis(tetrelcenes) **2a–c**, calculated at PBE0-D3/def2-TZVP (energies given in  $\text{kJ mol}^{-1}$ ).

## Experimental

### General

All manipulations were carried out under an argon inert gas atmosphere using Schlenk techniques or a glove box. Solvents were purified using an MBraun Solvent Purification System. NMR spectra were recorded on a Bruker Avance III 400 (solution) and a Bruker Avance III 400 WB (solid-state) spectrometers.  $^1\text{H}$  and  $^{13}\text{C}$  NMR spectra were referenced using the solvent signals,<sup>22</sup> and  $^{29}\text{Si}$  and  $^{119}\text{Sn}$  NMR spectra were refer-



enced using external standards ( $\delta^{29}\text{Si}(\text{SiMe}_4) = 0$ ;  $\delta^{119}\text{Sn}(\text{SnMe}_4) = 0$ ). A  $\text{Ca}^{119m}\text{SnO}_3$  source was used for the Mössbauer spectroscopic experiment on the **2c** sample. The measurement was carried out in a standard liquid nitrogen bath cryostat at 78 K. The source was kept at room temperature. The sample was mixed with alpha-quartz and enclosed in a small PMMA container at an optimized thickness.<sup>23</sup> Fitting of the data was done by using the WinNormos for Igor6 program package.<sup>24</sup> The FT-IR spectra of solid microcrystalline samples were recorded using attenuated total reflectance (ATR) on a Bruker Vertex 70 spectrometer. UV-Vis measurements were performed in quartz glass cuvettes with a 1 cm thickness. The spectra were recorded on a PerkinElmer Lambda 750 spectrometer equipped with an integrating sphere from 200 to 800 nm. Single crystal X-ray diffraction analysis was carried out on a Bruker D8 Venture diffractometer with a microfocus sealed tube and a Photon II detector using monochromated  $\text{CuK}\alpha$  radiation ( $\lambda = 1.54178 \text{ \AA}$ ). Structure solution and refinement with anisotropic displacement parameters of all non-hydrogen atoms were performed using SHELXL-2018/3 for **2c** and SHELXL-2019/1 for **2a** and **2b**.<sup>25</sup> Elemental analysis was performed on an Elementar Vario Micro Cube. Ligands **1a** and **1b** were prepared according to procedures known from the literature.<sup>26</sup> The  $\text{GeCl}_2$ -dioxane adduct and  $\text{SnCl}_2$  were purchased from ABCR and used as received.

### Synthesis and characterization of **2a-c**

**2a and 2c.** To a suspension of **1a** (for **2a**: 300 mg/1.17 mmol; for **2c**: 600 mg/2.34 mmol) in THF,  $\text{SnCl}_2$  (444 mg/2.34 mmol) or  $\text{GeCl}_2$ -dioxane (271 mg/1.17 mmol) in THF was added at room temperature, and the reaction mixture was stirred overnight. All volatiles were removed *in vacuo* and the residue was suspended in hexane and filtered. The removal of hexane *in vacuo* yielded **2a** and **2c** as colorless to light yellow solids.

**2a.** Crude yield: 167 mg/0.27 mmol/46%; crystalline yield: 49 mg/0.08 mmol/14%.

**$^1\text{H-NMR}$**  (400.13 MHz,  $\text{C}_6\text{D}_6$ , 296 K,  $\delta$  in ppm): 0.57 (s, 12H,  $\text{Si}(\text{CH}_3)_2$ ), 1.68 (s, 12H,  $\text{Cp-CH}_3$ ), 1.91 (s, 12H,  $\text{Cp-CH}_3$ ), 5.99 (m, 4H,  $\text{Cp-H}$ ), 6.38 (m, 4H,  $\text{Cp-H}$ ).

**$^{13}\text{C}\{^1\text{H}\}$ -NMR** (100.61 MHz,  $\text{C}_6\text{D}_6$ , 296 K,  $\delta$  in ppm): 1.7 ( $\text{Si}(\text{CH}_3)_2$ ), 9.9 ( $\text{Cp-CH}_3$ ), 13.5 ( $\text{Cp-CH}_3$ ), 107.5 ( $\text{C}^{\text{CP}}$ ), 117.8 ( $\text{C}^{\text{CP}}$ ), 121.5 ( $\text{C}^{\text{CP}}$ ), 123.8 ( $\text{C}^{\text{CP}}$ ), 125.7 ( $\text{C}^{\text{CP}}$ ), 126.9 ( $\text{C}^{\text{CP}}$ ).

**$^{29}\text{Si}\{^1\text{H}\}$ -NMR** (79.49 MHz,  $\text{C}_6\text{D}_6$ , 296 K,  $\delta$  in ppm): -20.0.

**CHN-analysis:** calculated for  $\text{C}_{32}\text{H}_{44}\text{Ge}_2\text{Si}_2$ : C: 61.00%, H: 7.04%; found: C: 60.91%, H: 7.45%.

**2c.** Crude yield: 471 mg/0.65 mmol/56%; crystalline yield: 277 mg/0.38 mmol/32%.

**$^1\text{H-NMR}$**  (400.13 MHz,  $\text{C}_6\text{D}_6$ , 293.1 K,  $\delta$  in ppm): 0.59 (s, 12H,  $\text{Si}(\text{CH}_3)_2$ ), 1.78 (s, 12H,  $\text{Cp-CH}_3$ ), 2.06 (s, 12H,  $\text{Cp-CH}_3$ ), 6.09 (m, 4H,  $\text{Cp-H}$ ), 6.45 (m, 4H,  $\text{Cp-H}$ ).

**$^{13}\text{C}\{^1\text{H}\}$ -NMR** (100.61 MHz,  $\text{C}_6\text{D}_6$ , 293 K,  $\delta$  in ppm): 2.2 ( $\text{Si}(\text{CH}_3)_2$ ), 10.0 ( $\text{Cp-CH}_3$ ), 13.9 ( $\text{Cp-CH}_3$ ), 107.6 ( $\text{C}^{\text{CP}}$ ), 119.9 ( $\text{C}^{\text{CP}}$ ), 122.8 ( $\text{C}^{\text{CP}}$ ), 124.8 ( $\text{C}^{\text{CP}}$ ).

**$^{29}\text{Si}\{^1\text{H}\}$ -NMR** (79.49 MHz,  $\text{C}_6\text{D}_6$ , 293 K,  $\delta$  in ppm): -20.4.

**$^{119}\text{Sn}\{^1\text{H}\}$ -NMR** (149.21 MHz,  $\text{C}_6\text{D}_6$ , 293 K,  $\delta$  in ppm): -2138.

**$^{119}\text{Sn}\{^1\text{H}\}$ -NMR** (149.27 MHz, CP/MAS(13 kH), 297 K,  $\delta$  in ppm):  $\delta_{\text{iso}} = -2143$ ,  $\delta_{11} = -2002$ ,  $\delta_{22} = -2098$ ,  $\delta_{33} = -2331$ .

**CHN-analysis:** calculated for  $\text{C}_{32}\text{H}_{44}\text{Si}_2\text{Sn}_2$ : C: 53.21%, H: 6.14%; found: C: 53.82%, H: 6.69%.

**2b.** A suspension of **1b** (300 mg/0.99 mmol) in THF was cooled to 195 K and a THF solution of  $\text{GeCl}_2$ -dioxane (231 mg/0.99 mmol) was added. The solution was warmed to room temperature and stirred overnight. All volatiles were removed *in vacuo*, and the residue was suspended in hexane and filtered. Hexane was removed *in vacuo* to obtain an orange solid. Colorless crystals could be obtained from a hexane/THF mixture.

Crude yield: 260 mg/0.36 mmol/72%. Crystalline yield: 59.0 mg/0.08 mmol/16%.

**$^1\text{H-NMR}$**  (400.13 MHz,  $\text{C}_6\text{D}_6$ , 293 K,  $\delta$  in ppm): 0.65 (s, 12H,  $\text{Si}(\text{CH}_3)_2$ ), 1.69 (s, 12H,  $\text{Cp-CH}_3$ ), 1.89 (s, 12H,  $\text{Cp-CH}_3$ ), 6.00 (m, 4H,  $\text{Cp-H}$ ), 6.31 (m, 4H,  $\text{Cp-H}$ ).

**$^{13}\text{C}\{^1\text{H}\}$ -NMR** (100.61 MHz,  $\text{C}_6\text{D}_6$ , 293 K,  $\delta$  in ppm): 0.8 ( $\text{Si}(\text{CH}_3)_2$ ), 9.89 ( $\text{Cp-CH}_3$ ), 13.2 ( $\text{Cp-CH}_3$ ), 107.0 ( $\text{C}^{\text{CP}}$ ), 111.0 ( $\text{C}^{\text{CP}}$ ), 119.4 ( $\text{C}^{\text{CP}}$ ), 120.0 ( $\text{C}^{\text{CP}}$ ), 122.9 ( $\text{C}^{\text{CP}}$ ), 124.9 ( $\text{C}^{\text{CP}}$ ).

**CHN-analysis:** calculated for  $\text{C}_{32}\text{H}_{44}\text{Ge}_4$ : C: 53.44%, H: 6.17%; found: C: 52.78%, H: 6.34%.

### Conflicts of interest

There are no conflicts to declare.

### Acknowledgements

Susanne Harling is thanked for elemental analysis. Lucas Niedner is thanked for IR spectroscopic measurements, and Anna Michaely and Max Briesenick are thanked for UV-Vis spectroscopic measurements. Instrumentation and technical assistance for this work were provided by the Service Center X-ray Diffraction, with financial support from Saarland University and the Deutsche Forschungsgemeinschaft.

### References

- 1 P. J. Davidson and M. F. Lappert, *J. Chem. Soc., Chem. Commun.*, 1973, 317a.
- 2 (a) D. E. Goldberg, D. H. Harris, M. F. Lappert and K. M. Thomas, *J. Chem. Soc., Chem. Commun.*, 1976, 261–262; (b) D. E. Goldberg, P. B. Hitchcock, M. F. Lappert, K. M. Thomas, A. J. Thorne, T. Fjeldberg, A. Haaland and B. E. R. Schilling, *J. Chem. Soc., Dalton Trans.*, 1986, 2387–2394; (c) J. Wiederkehr, C. Wölper and S. Schulz, *CCDC 1988449: Experimental Crystal Structure Determination*, 2020, DOI: [10.1107/ccdc.csd.cc24r4j1](https://doi.org/10.1107/ccdc.csd.cc24r4j1); (d) R. Sedlak, O. A. Stasyuk, C. F. Guerra, J. Řezáč, Al. Růžička and P. Hobza, *J. Chem. Theory Comput.*, 2016, 12, 1696–1704.
- 3 (a) P. P. Power, *Chem. Rev.*, 1999, 99, 3463–3503; (b) P. Jutzi, *Angew. Chem., Int. Ed. Engl.*, 1975, 14, 232–245.



4 (a) P. J. Davidson, D. H. Harris and M. F. Lappert, *J. Chem. Soc., Dalton Trans.*, 1976, 2268–2274; (b) P. B. Hitchcock, M. F. Lappert, S. J. Miles and A. J. Thorne, *J. Chem. Soc., Chem. Commun.*, 1984, 480–482.

5 For some selected examples see: (a) T. Tsumuraya, A. A. Batcheller and S. Masamune, *Angew. Chem.*, 1991, **103**, 916–944, (*Angew. Chem., Int. Ed. Engl.*, 1991, **30**, 902–930); (b) M. Driess and H. Grützmacher, *Angew. Chem.*, 1996, **108**, 900–929, (*Angew. Chem., Int. Ed. Engl.*, 1996, **35**, 828–856); (c) K. M. Baines and W. G. Stibbs, *Adv. Organomet. Chem.*, 1996, **39**, 275–320; (d) P. P. Power, *J. Chem. Soc., Dalton Trans.*, 1998, 2939–2951; (e) J. T. Snow, S. Murakami, S. Masamune and D. J. Williams, *Tetrahedron Lett.*, 1984, **25**, 4191–4194; (f) S. Masamune, Y. Hanzawa and D. J. Williams, *J. Am. Chem. Soc.*, 1982, **104**, 6136–6137; (g) J. Park, S. A. Batcheller and S. Masamune, *J. Organomet. Chem.*, 1989, **367**, 39–45; (h) S. A. Batcheller, T. Tsumuraya, O. Tempkin, W. M. Davis and S. Masamune, *J. Am. Chem. Soc.*, 1990, **112**, 9395–9397; (i) U. Lay, H. Pritzkow and H. Grützmacher, *J. Chem. Soc., Chem. Commun.*, 1992, 260–262; (j) K. W. Klinkhammer and W. Schwarz, *Angew. Chem., Int. Ed. Engl.*, 1995, **34**, 1334–1336; (k) M. Weidenbruch, H. Kilian, K. Peters, H. G. von Schnering and H. Marsmann, *Chem. Ber.*, 1995, **128**, 983–985; (l) P. Jutzi, H. Schmidt, B. Neumann and H.-G. Stammler, *Organometallics*, 1996, **15**, 741–746; (m) M. Kira, T. Iwamoto, T. Maruyama, C. Kabuto and H. Sakurai, *Organometallics*, 1996, **15**, 3767–3769; (n) A. Schäfer, W. Saak, M. Weidenbruch, H. Marsmann and G. Henkel, *Chem. Ber.*, 1997, **130**, 1733–1737; (o) K. W. Klinkhammer, T. F. Fässler and H. Grützmacher, *Angew. Chem., Int. Ed.*, 1998, **37**, 124–126; (p) H. Schäfer, W. Saak and M. Weidenbruch, *Organometallics*, 1999, **18**, 3159–3163; (q) G. Ramaker, W. Saak, D. Haase and M. Weidenbruch, *Organometallics*, 2003, **22**, 5212–5216; (r) K. Kishikawa, N. Tokitoh and R. Okazaki, *Chem. Lett.*, 1998, **27**, 239–240; (s) W. Ando, T. Tsumuraya and A. Sekiguchi, *Chem. Lett.*, 1987, **16**, 317–318; (t) L. Klemmer, A.-L. Thömmes, M. Zimmer, V. Huch, B. Morgenstern and S. Scheschkewitz, *Nat. Chem.*, 2021, **13**, 373–377.

6 (a) T. J. Hadlington, M. Hermann, J. Li, G. Frenking and C. Jones, *Angew. Chem., Int. Ed.*, 2013, **52**, 10199–10203; (b) T. Sasamori, Y. Sugiyama, N. Takeda and N. Tokitoh, *Organometallics*, 2005, **24**, 3309–3314; (c) G. H. Spikes, J. C. Fettinger and P. P. Power, *J. Am. Chem. Soc.*, 2005, **127**, 12232–11223; (d) M. Weidenbruch, M. Stürmann, H. Kilian, S. Pohl and W. Saak, *Chem. Ber.*, 1997, **130**, 735–738.

7 (a) D. H. Harris and M. F. Lappert, *J. Chem. Soc., Chem. Commun.*, 1974, 895–896; (b) R. W. Chorley, P. B. Hitchcock, M. F. Lappert, W.-P. Leung, P. P. Power and M. M. Olmstead, *Inorg. Chim. Acta*, 1992, **198–200**, 203–209; (c) T. Fjeldberg, H. Hope, M. F. Lappert, P. P. Power and A. J. Thorne, *J. Chem. Soc., Chem. Commun.*, 1983, 639–641; (d) M. Veith, *Angew. Chem.*, 1975, **87**, 287–288, (*Angew. Chem., Int. Ed.*, 1975, **14**, 263–264); (e) M. Veith, *Z. Naturforsch., B: Anorg. Chem., Org. Chem.*, 1978, **33**, 1.

8 (a) M. A. Beswick, J. S. Palmer and D. S. Wright, *Chem. Soc. Rev.*, 1998, **27**, 225–232; (b) P. Jutzi and N. Buford, *Chem. Rev.*, 1999, **99**, 969–990.

9 (a) E. O. Fischer and H. Grubert, *Z. Anorg. Allg. Chem.*, 1956, **5–6**, 237–242; (b) E. O. Fischer and H. Grubert, *Z. Naturforsch., B: Anorg. Chem., Org. Chem., Biochem., Biophys., Biol.*, 1956, **11**, 423–424.

10 J. V. Scibelli and M. D. Curtis, *J. Am. Chem. Soc.*, 1973, **95**, 924–925.

11 (a) J. N. Jones, J. A. Moore, A. H. Cowley and C. L. B. Macdonald, *Dalton Trans.*, 2005, **24**, 3846–3851; (b) M. Schleep, C. Hettich, J. V. Rojas, D. Kratzert, T. Ludwig, K. Lieberth and I. Krossing, *Angew. Chem., Int. Ed.*, 2017, **56**, 2880–2884; (c) M. Schorpp and I. Krossing, *Chem. – Eur. J.*, 2020, **26**, 14109–14117.

12 C. Müller, A. Stählich, L. Wirtz, C. Gretsch, V. Huch and A. Schäfer, *Inorg. Chem.*, 2018, **57**, 8050–8053.

13 (a) J. Park, Y. Seo, S. Cho, D. Whang, K. Kim and T. Chang, *J. Organomet. Chem.*, 1995, **489**, 23–25; (b) D. L. Zechel, S. A. Foucher, J. K. Pudelski, G. P. A. Yap, A. L. Rheingold and I. Manners, *J. Chem. Soc., Dalton Trans.*, 1995, 1893–1899; (c) M. Herberhold and T. Bärtl, *Z. Naturforsch., B: J. Chem. Sci.*, 1995, **50**, 1692–1698; (d) T. Baumgartner, F. Jäkle, R. Rulkens, G. Zech, A. J. Lough and I. Manners, *J. Am. Chem. Soc.*, 2002, **124**, 10062–10070.

14 G. K. Anderson and N. P. Rath, *J. Organomet. Chem.*, 1991, **414**, 129–135.

15 (a) B. Wrackmeyer, A. Sebald and L. H. Merwin, *Magn. Reson. Chem.*, 1991, **29**, 260–263; (b) I.-A. Bischoff, B. Morgenstern and A. Schäfer, *Chem. Commun.*, 2022, **58**, 8934–8937.

16 Satellites with a coupling constant of 7165 Hz are observed in the  $^{119}\text{Sn}\{^1\text{H}\}$ (CP/MAS) NMR spectrum, which we tentatively assigned to a  $^1\text{J}(^{119}\text{Sn}–^{117}\text{Sn})$  coupling.

17 (a) **2a**: Ge–Cp<sup>cent</sup>: 230.87(2) pm/Ge–Cp<sup>#cent</sup>: 214.71(2) pm; **2b**: Ge–Cp<sup>cent</sup>: 230.78(3) pm/Ge–Cp<sup>#cent</sup>: 215.34(2) pm; Si[2]germanocenophanes: Ge–Cp<sup>cent</sup>: 224.19(5) pm to 225.07(5) pm (ref. 18a)/Ge–Cp<sup>#cent</sup>: 220.94(2) pm to 222.51(2) pm. <sup>18b</sup> (b) **2c**: Sn–Cp<sup>cent</sup>: 245.71(3) pm; Sn–Cp<sup>#cent</sup>: 235.92(4) pm; Si[2]stannocenophanes: Sn–Cp<sup>cent</sup>: 239.42(3) pm to 242.36(3) pm (ref. 18a)/Sn–Cp<sup>#cent</sup>: 240.91(3) pm to 241.17(3) pm. <sup>18b</sup>

18 (a) A. Schäfer, K. Rohe, A. Grandjean and V. Huch, *Eur. J. Inorg. Chem.*, 2017, 35–38; (b) A. S. D. Stählich, V. Huch, A. Grandjean, K. Rohe, K. Leszczynska, D. Scheschkewitz and A. Schäfer, *Chem. – Eur. J.*, 2019, **25**, 173–176.

19 M. Mantina, A. C. Chamberlin, R. Valero, C. J. Cramer and D. G. Truhlar, *J. Phys. Chem. A*, 2009, **113**, 5806–5812.

20 P. G. Harrison and J. J. Zuckerman, *J. Am. Chem. Soc.*, 1969, **91**, 6885–6886.

21 See the ESI for further details.†

22 G. R. Fulmer, A. J. M. Miller, N. H. Sherden, H. E. Gottlieb, A. Nudelman, B. M. Stoltz, J. E. Bercaw and K. I. Goldberg, *Organometallics*, 2010, **29**, 2176–2179.

23 G. J. Long, T. E. Cranshaw and G. Longworth, *Moessbauer Eff. Ref. Data J.*, 1983, **6**, 42–49.

24 R. A. Brand, *WinNormos for Igor6 (version for Igor 6.2 or above: 22/02/2017)*, Universität Duisburg, Duisburg (Germany), 2017.

25 (a) G. M. Sheldrick, *Acta Crystallogr., Sect. A: Found. Crystallogr.*, 2008, **64**, 112–122; (b) G. M. Sheldrick, *Acta Crystallogr., Sect. A: Found. Adv.*, 2015, **71**, 3–8; (c) C. B. Hübschle, G. M. Sheldrick and B. Dittrich, *J. Appl. Crystallogr.*, 2011, **44**, 1281–1284.

26 (a) P. Beagley, P. Davies, H. Adams and C. White, *Can. J. Chem.*, 2011, **79**, 731–741; (b) D. Stern, M. Sabat and T. J. Marks, *J. Am. Chem. Soc.*, 1990, **112**, 9558–9575; (c) C. Alonso-Moreno, A. Antíñolo, I. López-Solera, A. Otero, S. Prashar, A. M. Rodríguez and E. Villaseñor, *J. Organomet. Chem.*, 2002, **656**, 129–138; (d) P. Jutzi and R. Dickbreder, *Chem. Ber.*, 1986, **119**, 1750–1754; (e) H. Schumann, L. Esser, J. Loebel, A. Dietrich, D. Van der Helm and W. Ji, *Organometallics*, 1991, **10**, 2585–2592.

